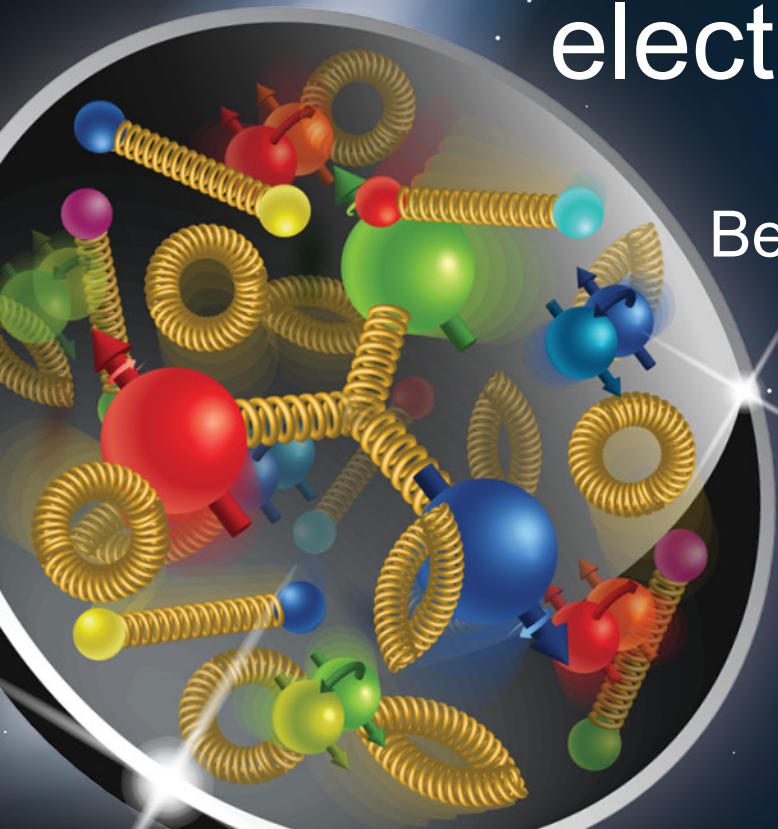


Proton beam emittance growth due to due strongly disrupted electron beam in eRHIC



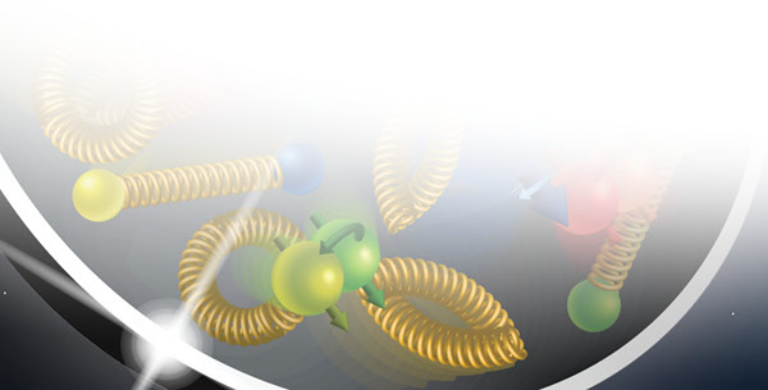
Beam-Beam Effects in Circular Colliders
Berkeley, 5-7 February 2018

G. Bassi*, Y. Hao, A. He, Y. Luo,
C. Montag, V. Smaluk, F. Willeke

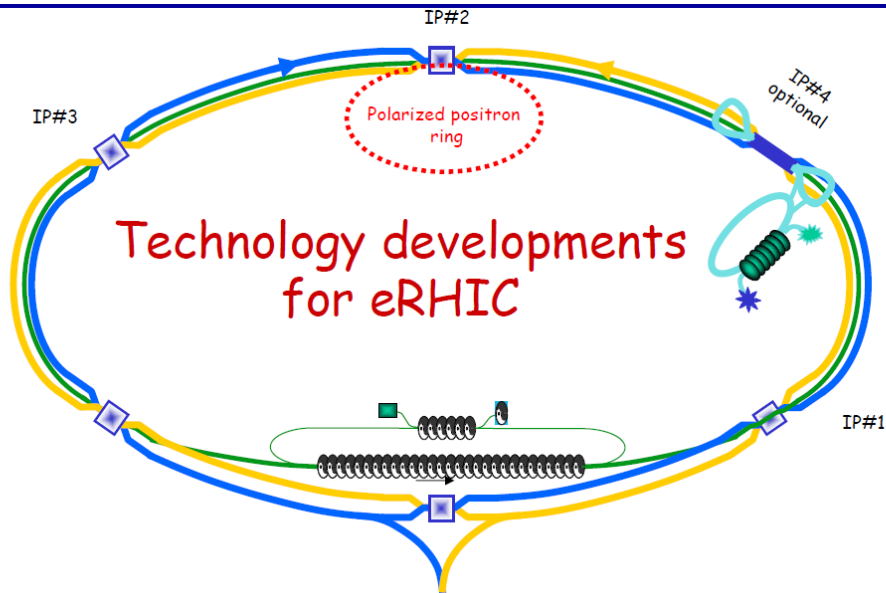
Electron Ion Collider – eRHIC

Outline

- **Linac Ring eRHIC and beam-beam effects**
- **Strong-strong beam beam simulations with BBSS (K. Ohmi):**
 - **Electron beam disruption.**
 - **Proton beam emittance growth due to fluctuations of the electron bunch centroid at the interaction point (IP).**
- **Discussion/future studies**



Linac-Ring eRHIC



Technology developments
for eRHIC

Vladimir N. Litvinenko for eRHIC team

Collider Accelerator Department, Brookhaven National Laboratory, Upton, NY, USA



Annual DOE/Nuclear Physics Review of RHIC Science and Technology, Vladimir Litvinenko, July 25, 2006



Appendix A of the eRHIC ZDR

Linac-Ring eRHIC.

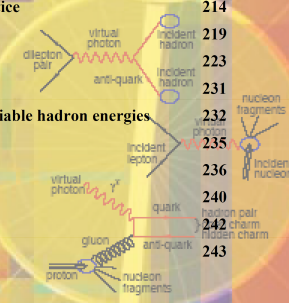
Daniel Anderson, Ilan Ben-Zvi¹, Rama Calaga¹, Xiangyun Chang¹,
Manouchehr Farkhondeh², Alexei Fedotov¹, Jörg Kewisch¹, Vladimir Litvinenko¹,
William Mackay¹, Christoph Montag¹, Thomas Roser¹, Vitaly Yakimenko³

⁽¹⁾ C-AD, BNL, ⁽²⁾ Bates, MIT, ⁽³⁾ Physics Department, BNL

Content

page

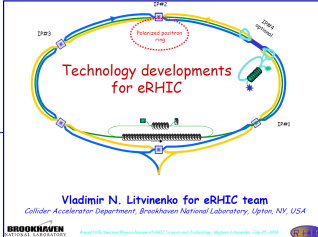
1. Introduction to the Linac-Ring collider	173
1.1 Advantages of the ERL-based eRHIC	181
2. Main beam parameters and luminosity	183
3. Layout of the Linac-ring eRHIC	186
a. Energy recovery Linac	188
b. Polarized electron gun	204
c. Laser source for the polarized gun	209
d. The e-beam polarization and polarization transparency of the ERL lattice	214
e. Electron cooling	219
f. Integration with IP	223
g. Considerations of the experiments	231
h. Adjustment of collision frequency for variable hadron energies	232
4. Cost	235
5. R&D items	236
6. Future energy upgrades	240
7. Summary	242
8. Acknowledgements	243



Linac-Ring eRHIC Design

my highlight

Linac-Ring Design based on 5-20+ GeV ERL



IP#10 - optional

IP#12 - main

Electron cooling

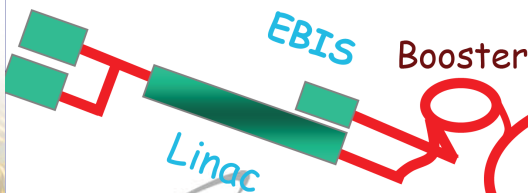
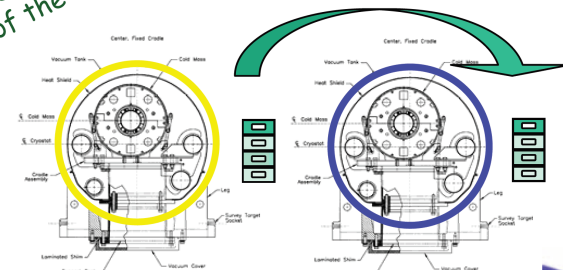
- Polarized electrons are generated in a gun, accelerated, put into collision(s), decelerated and dumped inside superconducting energy recovery linac (ERL).
- No beam-beam limitation for electron beam (the beam is used once!).
- No prohibited energy areas for the polarization.
- No spin rotators needed
- No trade-offs between detector length and luminosity
- e^-p luminosity up to $10^{34} \text{ cm}^{-2}\text{s}^{-1}$
- Polarized positrons are possible only with additional ring

Ø1.22 km

IP#4- optional

RHIC

For multiple passes:
vertical separation of the arcs



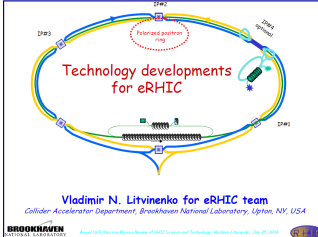
AGS

BROOKHAVEN
NATIONAL LABORATORY

Annual DOE Nuclear Physics Review of RHIC Science and Technology, Vladimir Litvinenko, July 25, 2006



Linac-Ring eRHIC: Round Beams



In linac-ring eRHIC luminosity is determined by the hadron beam!

$$L = f_c \frac{N_e N_h}{4 \pi \beta_h^* \epsilon_h}$$

Round beams $\beta_e^* \epsilon_e = \beta_h^* \epsilon_h$

$$L = \gamma_h \cdot (f_c \cdot N_h) \cdot \frac{\xi_h \cdot Z_h}{\beta_h^* \cdot r_h}$$

In parallel with STAR and PHENIX

$$\xi_h = \frac{N_e}{\gamma_h} \frac{r_h}{4 \pi Z \epsilon_h} = 0.007$$



Luminosity $10^{33} \text{ cm}^{-2} \text{ sec}^{-1}$	<i>Protons</i> 26 GeV	<i>Protons</i> 50 GeV	<i>Protons</i> 100 GeV	<i>Protons</i> 250 GeV
<i>Electrons</i> 5(2)-10(20) GeV	0.28	0.52	0.96	2.8
Luminosity (per nucleus) $10^{31} \text{ cm}^{-2} \text{ sec}^{-1}$	<i>Au</i> 50 GeV/u	<i>Au</i> 100 GeV/u		
<i>Electrons</i> 5(2)-10(20) GeV	1.4	2.8		

Dedicated eRHIC mode with 250 GeV p or 100 GeV/u Au

$$\xi_h \rightarrow 0.02 \quad \Leftrightarrow \quad L_{p e} \rightarrow 1 \cdot 10^{34}$$

Electron Disruption

PHYSICAL REVIEW SPECIAL TOPICS - ACCELERATORS AND BEAMS **13**, 071003 (2010)

Effect of electron disruption in the energy recovery linac based electron ion collider

Y. Hao and V. Ptitsyn

Brookhaven National Laboratory, Upton, New York 11973, USA

(Received 2 February 2010; published 19 July 2010)

Beam-beam effects present one of the major factors limiting the luminosity of colliders. In the energy recovery linac (ERL) based eRHIC design, the electron beam, accelerated in a superconducting ERL, collides with the proton beam circulating in the RHIC ring. During such collisions the electron beam undergoes a very strong beam-beam interaction with the protons, which warrants careful examination. We evaluated transverse disruption and linear mismatch effects in the electron beam caused by collisions and considered several countermeasures to mitigate the emittance growth from these interactions. The minimum required aperture of transport lines is calculated that should allow the transport of the electron beam during the deceleration process.

TABLE I. ERL-based eRHIC beam parameters.

	High-energy setup		Low-energy setup	
	p	e	p	e
Energy (GeV)	250	10	50	3
Number of bunches	166		166	
Bunch intensity (10^{11})	2.0	1.2	2.0	1.2
Beam current (mA)	420	260	420	260
95% normalized emittance (π mm mrad)	6	115	6	115
rms emittance (nm rad)	3.8	1.0/(5.0)	19.0	3.3/(16.5)
β^* (cm)	26	100/(20)	26	150/(30)
Beam-beam parameter	0.015	2.3/(0.46)	0.015	2.3 (0.46)
Disruption parameter	0.005	5.8	0.01	3.8
rms bunch length (cm)	20	0.7	20	1.5
Polarization (%)	70	80	70	80
Peak luminosity (10^{33} cm $^{-2}$ s $^{-1}$)		2.6		0.53

Beam-Beam Strong-Strong Code

Particle In Cell

- Beam potential

$$G(x, y) = \frac{1}{2} \ln(x^2 + y^2)$$

$$\phi(x) = -\frac{2Nr_e}{\gamma} \int dx' G(x - x') \rho(x')$$

$$\text{Inte} G(x_i, y_j) = \int_{y_j - \Delta y/2}^{y_j + \Delta y/2} \int_{x_i - \Delta x/2}^{x_i + \Delta x/2} G(x, y) dx dy$$

$$g(x, y) \equiv \int \int \log(x^2 + y^2) dx dy = -3xy + x^2 \tan^{-1}(y/x) + y^2 \tan^{-1}(x/y) + xy \log(x^2 + y^2)$$

Chromaticity

- Effective Hamiltonian/generating function at IP.

$$H_I(x, \bar{p}, \delta) = \sum_{n=1} \frac{a_n x^2 + 2b_n x \bar{p} + c_n \bar{p}^2}{2} \delta^n$$

Relations between a,b,c and chromaticity, ν', α', β' .

Transformation for chromaticity

$$a_1 = \frac{\sin^2 \mu_0}{\beta_0^2} [-\beta_1 (\cot \mu_0 + \alpha_0) (1 + \alpha_0^2) + \{-\alpha_1 + \mu_1 \csc^2 \mu_0 + 2\alpha_1 \alpha_0 \cot \mu_0 + (\alpha_1 + \mu_1 \csc^2 \mu_0 \alpha_0^2) \beta_0\}],$$

$$b_1 = \frac{\sin^2 \mu_0}{\beta_0} [-\beta_1 (1 + \alpha_0^2) + \{\alpha_1 \cot \mu_0 + (\alpha_1 + \mu_1 \csc^2 \mu_0) \alpha_0\} \beta_0],$$

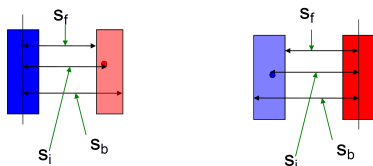
$$c_1 = [\beta_1 \cot \mu_0 - \beta_1 \alpha_0 + (\alpha_1 + \mu_1 \csc^2 \mu_0) \beta_0] \sin^2 \mu_0$$

$$\mu = \mu_0 + \mu_1 \delta, \beta = \beta_0 + \beta_1 \delta \text{ and } \alpha = \alpha_0 + \alpha_1 \delta$$

&HERING

chrhm=0.5,-48,-17.7,1.5,81.5,-0.609

3D symplectic integrator for slice-by-slice collision



- Since the interaction depends on z, energy kick should be taken into account $d\phi/dz$.

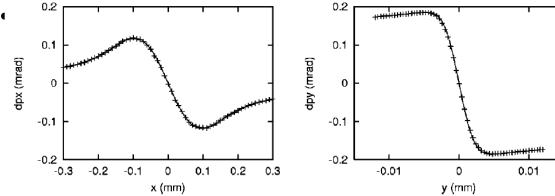
- We repeat the same procedure exchanging particle and slice

BBSS

K. Ohmi, KEK

Beam-beam force for flat beam

- Integrated Green function is indispensable to reproduce correct beam-beam force for flat beam, $\sigma_x/\sigma_y > 100$.



Crossing angle, crab cavity

- Crossing angle is equivalent to collision of two beams with xz tilt.

$$H = \pm \theta_{crs} p_x z \delta(s - s^*)$$

$$x = \tan \theta_{crs} z + \left(1 + \frac{p_x}{p_s} \sin \theta_{crs}\right) x$$

$$y = y + \sin \theta_{crs} \frac{p_y}{p_s} x$$

$$z = \frac{z}{\cos \theta_{crs}} - \frac{H}{p_s} \sin \theta_{crs}$$

$$\bar{p}_x = \frac{p_x - \tan \theta_{crs} H}{\cos \theta_{crs}}$$

$$\bar{p}_y = \frac{p_y}{\cos \theta_{crs}}$$

$$p_s = p_s - \tan \theta_{crs} p_x + \tan^2 \theta_{crs} H$$

$$H = (1 + p_x) - \sqrt{(1 + p_x)^2 - p_x^2 - p_y^2}$$

$$p_s = \sqrt{(1 + p_x)^2 - p_x^2 - p_y^2}$$

xz tilt can be controlled by crab cavity.

$$\frac{eV_{crab} \omega_{crab}}{cE_0} \sqrt{\beta_x^* \beta_{x,crab}} = \theta_{crs}$$

$$H = \frac{eV_{crab}}{E_0} x \sin\left(\frac{\omega_{crab} z}{c}\right) \delta(s - s_{crab})$$

$$H_{eff}^* = \frac{c\theta_{crb}}{\omega_{crb}} p_x \sin\left(\frac{\omega_{crb} z}{c}\right) \delta(s - s^*)$$

K. Ohmi, Phys. Rev E 62, 5 (2000)

Arc transformation

- Linear transfer matrix (6x6)

$$M_{2 \times 2 \times 2} = \begin{pmatrix} M_x & 0 & 0 \\ 0 & M_y & 0 \\ 0 & 0 & M_z \end{pmatrix} \quad M_i(s) = \begin{pmatrix} \cos \mu_i + \alpha_i \sin \mu_i & \beta_i \sin \mu_i \\ -\gamma_i \sin \mu_i & \cos \mu_i - \alpha_i \sin \mu_i \end{pmatrix}$$

- Take into account of dispersion and x-y coupling at IP

$$M_6 = R_{\eta} M_{4 \times 2} R_{\eta}^{-1} \quad R_{\eta} = \begin{pmatrix} (1 - \frac{|\beta_{x,y}|}{1 + \alpha_{x,y}^2}) I_2 & \frac{\beta_{x,y} S_2 R_{12}^T S_2}{1 + \alpha_{x,y}^2} & R_{\eta,x} \\ \frac{\beta_{x,y} S_2 R_{12}^T S_2}{1 + \alpha_{x,y}^2} & (1 - \frac{|\beta_{x,y}|}{1 + \alpha_{x,y}^2}) I_2 & R_{\eta,y} \\ S_2 R_{12}^T S_2 & r_{3,0} I_2 & r_{3,0} I_2 \end{pmatrix}$$

- Crabbing and crossing angle, ζ

$$R_{\eta,i} = \begin{pmatrix} \zeta_i & \eta_i \\ \zeta_i' & \eta_i' \end{pmatrix} \quad i = x, y$$

- Important parameters $R = \begin{pmatrix} r_{01} I_2 & -S_2 R_{12}^T S_2 \\ -R_2 & r_{01} I_2 \end{pmatrix} \quad R_2 = \begin{pmatrix} r_{11} & r_{12} \\ r_{21} & r_{22} \end{pmatrix}$

Flat beam β_x, α_y (waist), $\beta_y, \nu_x, \nu_y, \eta_x, \eta_y, r_{1-4}, \zeta_x$ (crab angle),

Round beam + η_x, η_y, α_x twiss=0, 2, 34.08, 0, 0.07, 31.09, 0, 8., 0.025, 0.0, 0.0, 0.0, 0.0, 0.0, 0.0, 0.0, 0.0, 0.0

3D beam-beam interaction



Strong-strong

- $\beta_y = 1\text{mm}$, $\sigma_z = 2.3(\text{LEP3}) - 1.7(\text{TLEP-h})\text{mm}$. For $\sigma_z > \beta_y$, the beam-beam force varies significantly along the bunch length.

- A bunch is divided into several slices which contain many macro-particles.

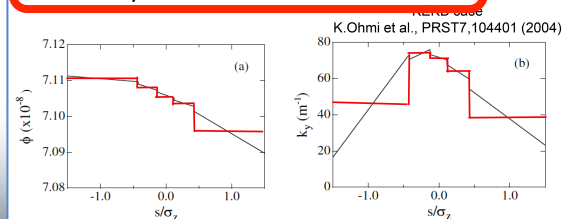
- Collision is calculated slice by slice.

$$\prod_{i=1}^{N_{d,s}} \exp[-V_{0,+}^{-1}(s_{-i}) \phi_{-i}(+, s_{-i}) V_{0,+}(s_{-i}) \Delta s] \quad \text{drift between slices}$$

$$V_0(s) = V_0(s, 0) = S \exp[-\int_0^s H ds']$$

$$\prod_{i=1}^{N_{d,s}} \exp[-V_{0,-}^{-1}(s_{+j}) \phi_{+j}(-, s_{+j}) V_{0,-}(s_{+j}) \Delta s] = \prod_{i=1}^{N_{d,s}} \exp[-\int_0^s H ds']$$

Potential and linear kick of the slice-by-slice collision



$$\phi_j(s) = \phi_j(s_b) + \frac{\phi_j(s_f) - \phi_j(s_b)}{s_f - s_b} (s - s_b)$$

$$\phi_j(s) = \phi_j(s_c)$$

$$k_y = \partial^2 \phi(s) / \partial y^2 = \Delta p_y / \Delta x$$

- potential is interpolated.

- potential at center of slice, BAD method

eRHIC Beam-Beam Simulations with BBSS

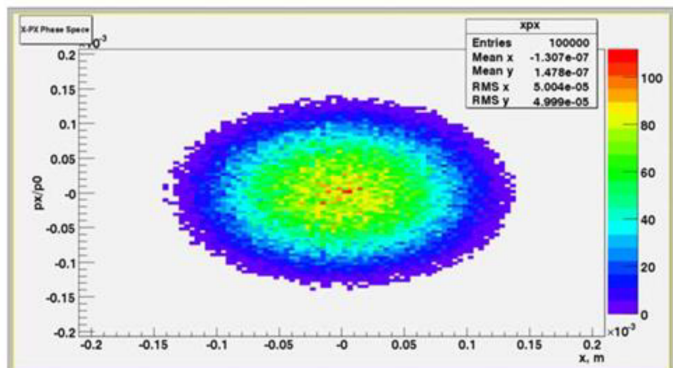
Machine and Beam Parameters Linac-Ring Option*

	Unit	protons	electrons
Circumference	m	3833.845	
Energy	GeV	250	10
Bunch population	10^{11}	1	1.2
Number of bunches		330	
Emittance	nm	3.8	5.0
Beta at IP	m	0.26	0.2
Bunch length	cm	20	0.7
Beam-beam parameter		0.015	0.23
Betatron tune		31.310/32.305	
Synchrotron tune		0.002	0.025
Radiation damping time	ms		25.5/51
Energy spread		0.0007	0.0005
Luminosity	$10^{33} \text{ cm}^{-2}\text{s}^{-1}$		2.7

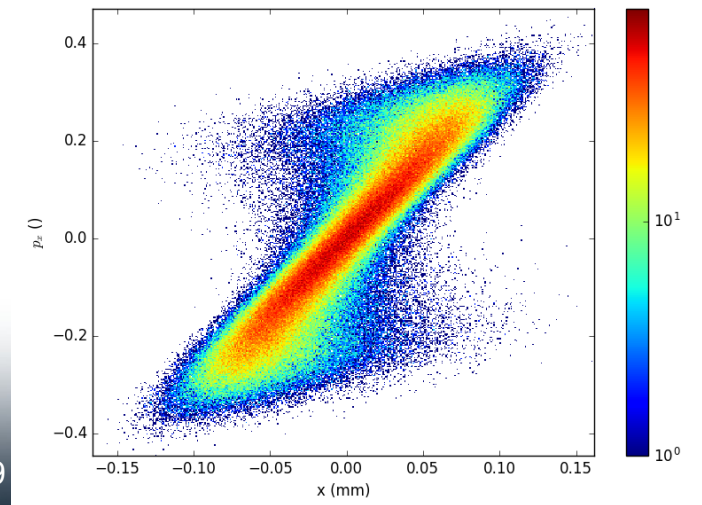
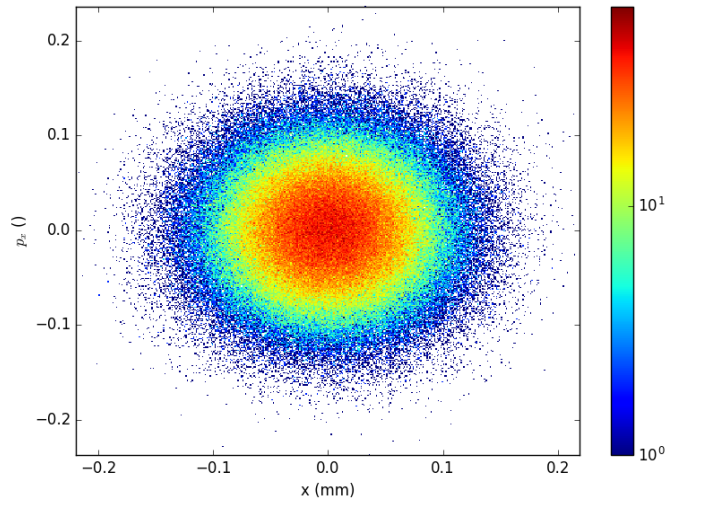
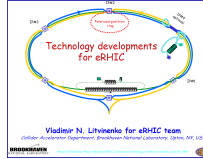
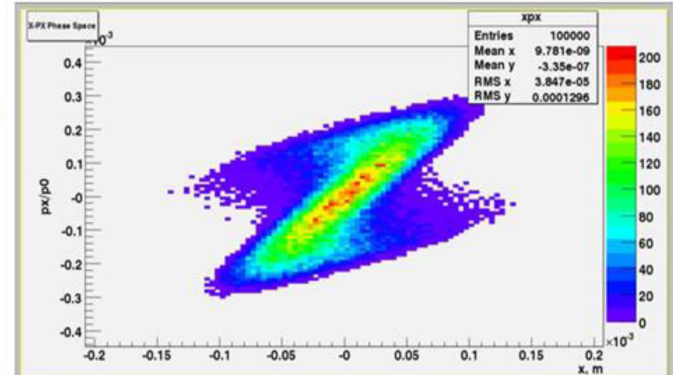
* Phys. Rev. ST Accel. Beams **13**, 071003 (2010)

Comparing Electron Disruption ($\beta_e^* = 1m, \epsilon_e = 2.5nm$)

Beam Disruption -LINAC-RING (Y. Hao)



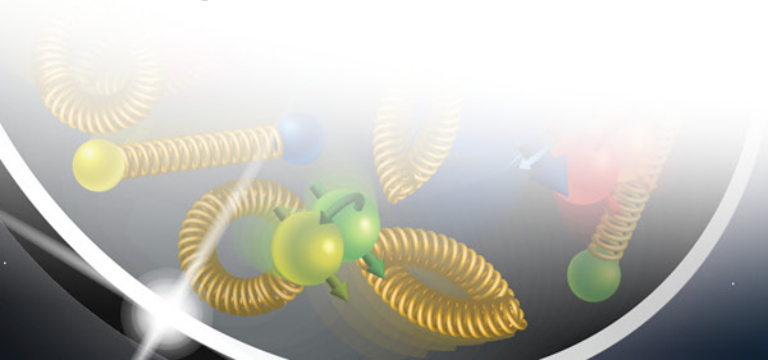
Interaction



BBSS

BBSS simulations with random offsets in e-beam

- **Centroid of freshly injected e-bunch perturbed by randomly generated offsets(x/y) at IP.**
- **Offsets normally distributed with zero mean and standard deviation σ_{offs} .**
- **Effect of random offsets studied by calculating growth rates of proton bunch size.**

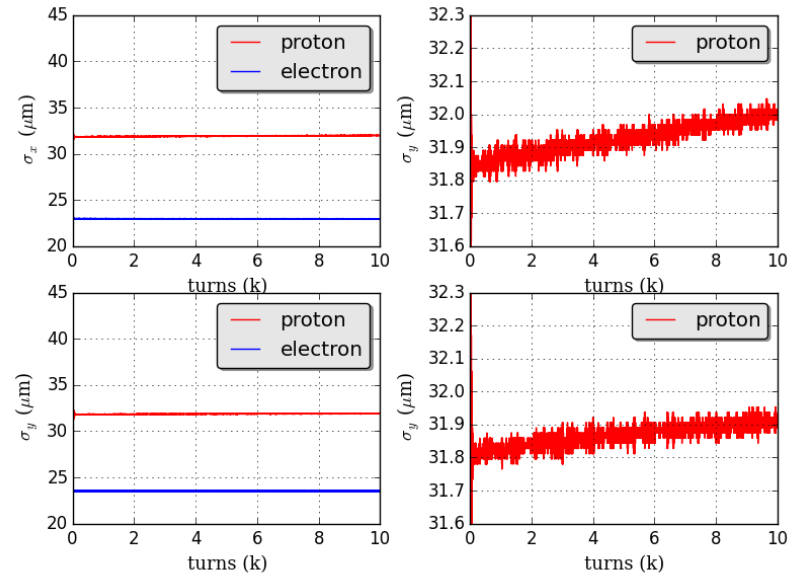
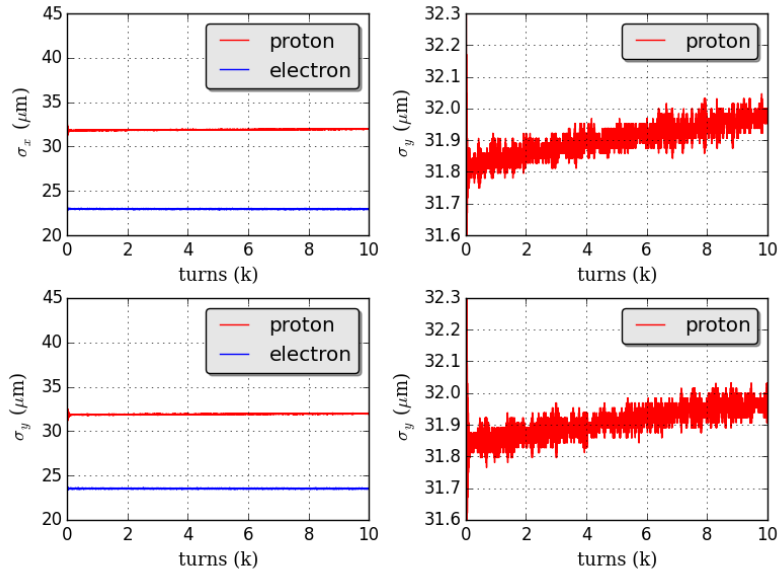


BBSS simulations without random offsets in e-beam

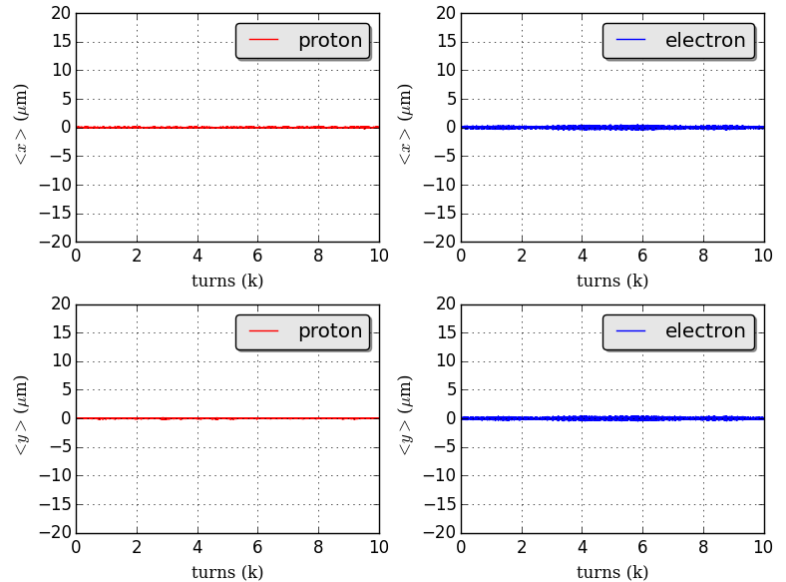
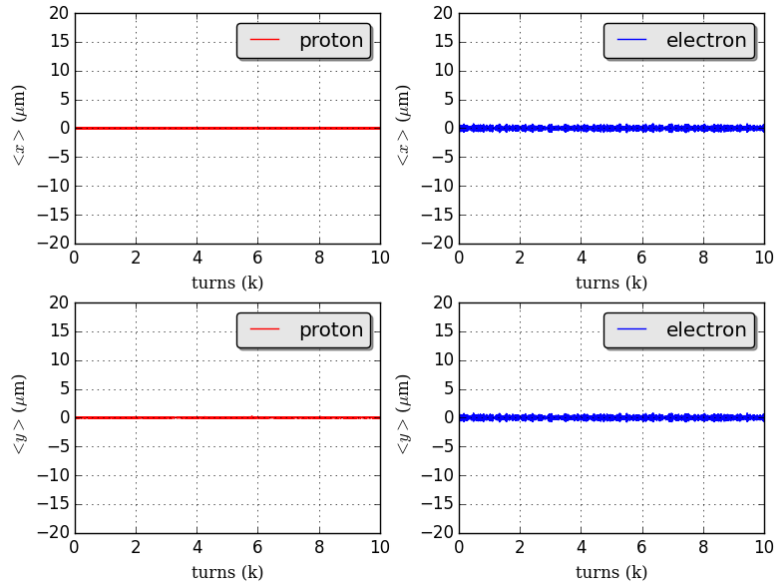
$M_p = M_e = 500k$

M # of macroparticles

$M_p = N_e = 1M$



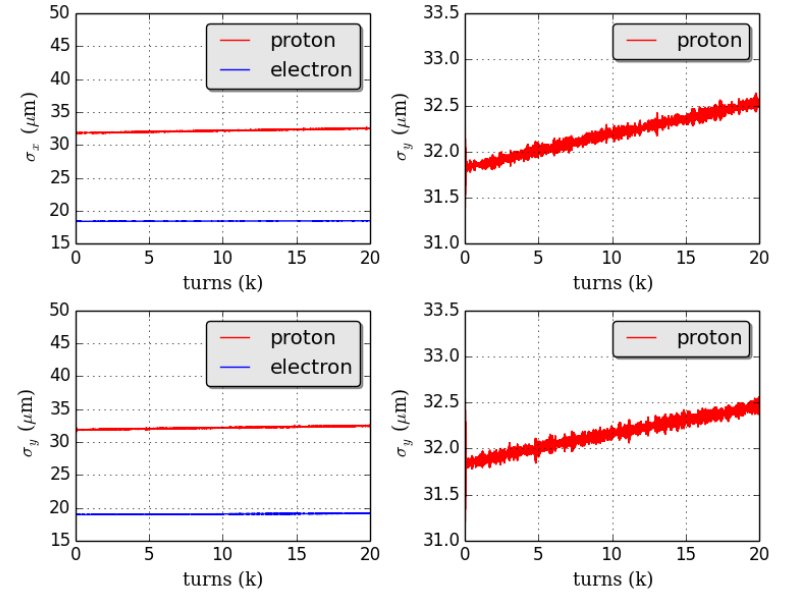
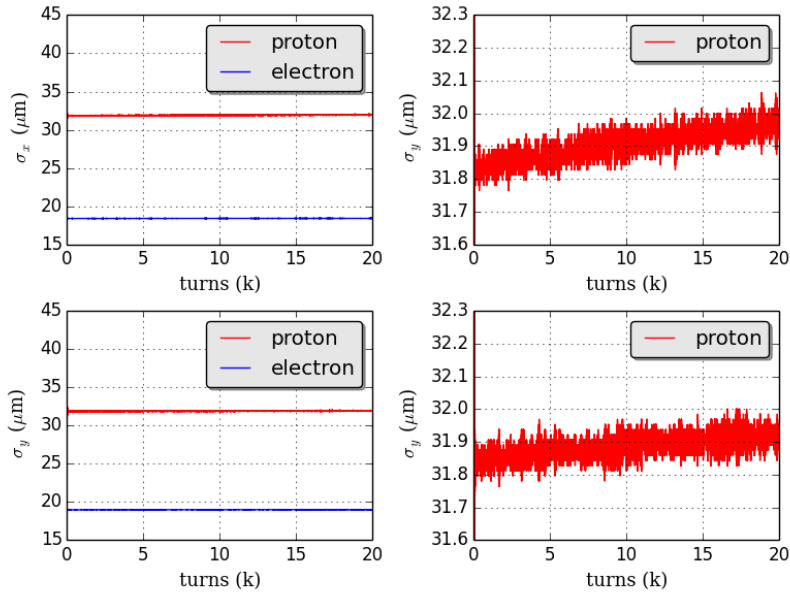
similar proton size growth rates: $g_{x,p} \approx 0.2 \mu\text{m/s}$, $g_{y,p} \approx 0.1 \mu\text{m/s}$



BBSS simulations with random offsets in e-beam

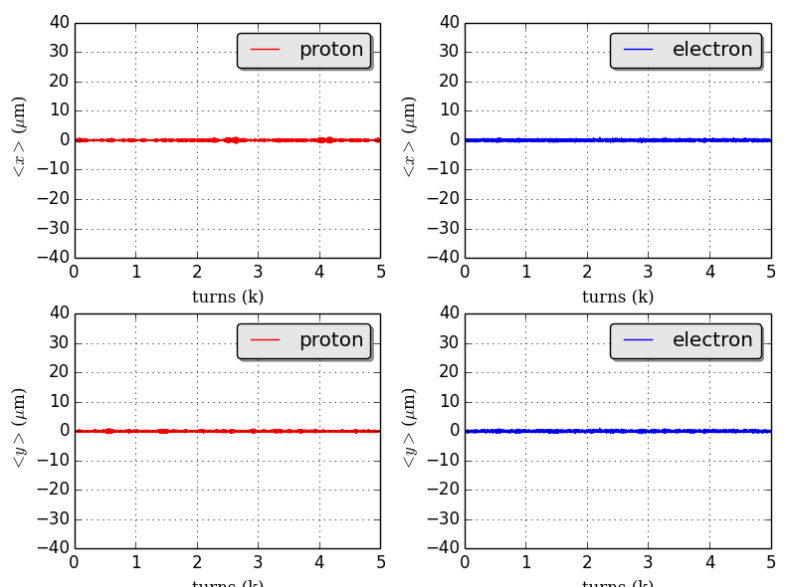
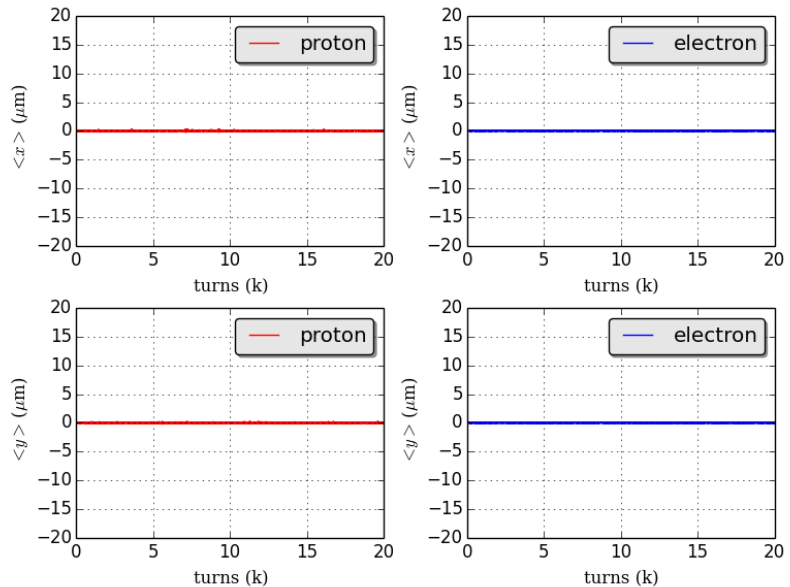
$\sigma_{\text{offs}} = 0.03 \mu\text{m}$

$\sigma_{\text{offs}} = 0.5 \mu\text{m}$



$g_{x,p} \approx 0.2 \mu\text{m/s}$, $g_{x,p} \approx 0.1 \mu\text{m/s}$

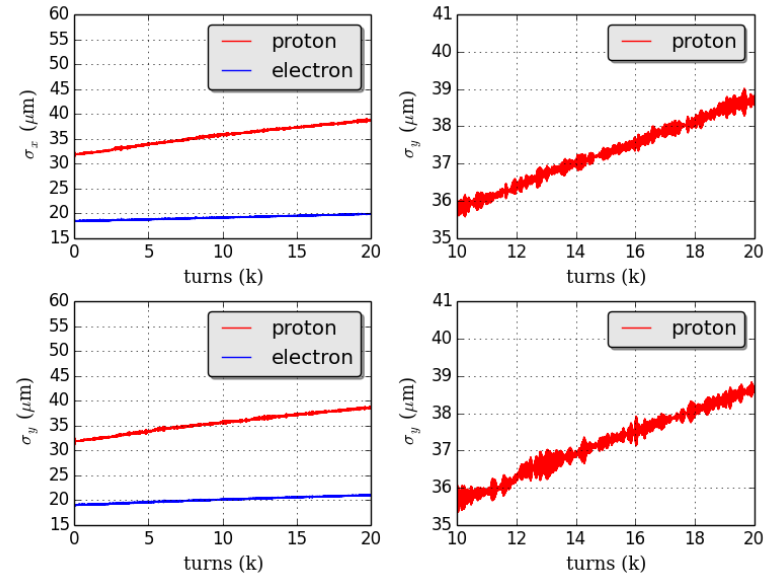
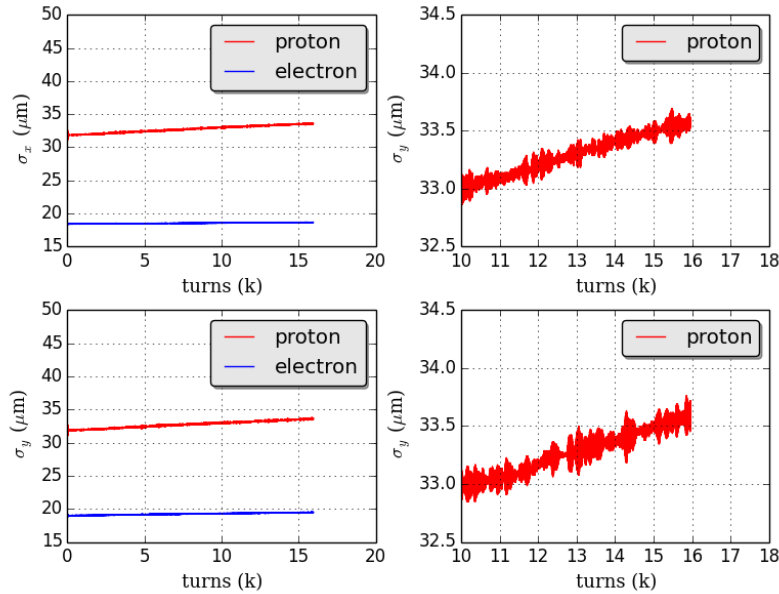
$g_{x,p} \approx 1.0 \mu\text{m/s}$, $g_{x,p} \approx 0.9 \mu\text{m/s}$



BBSS simulations with random offsets in e-beam

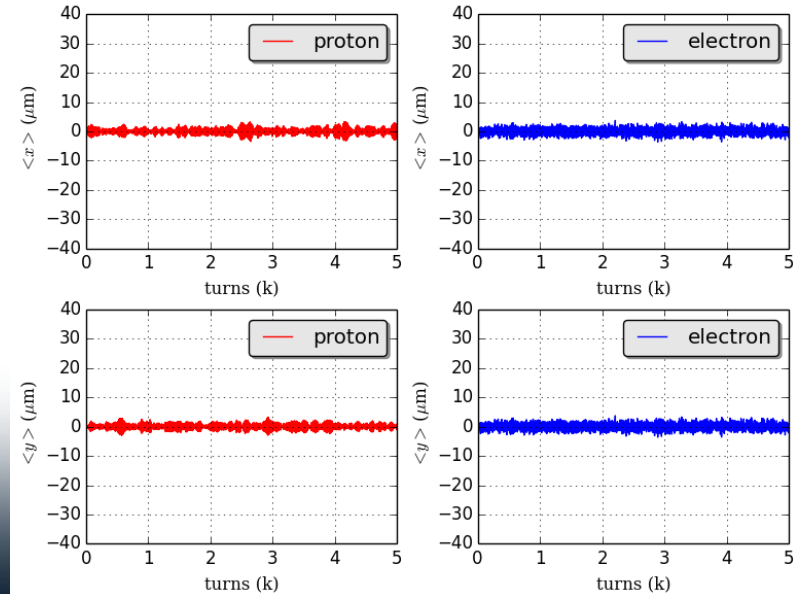
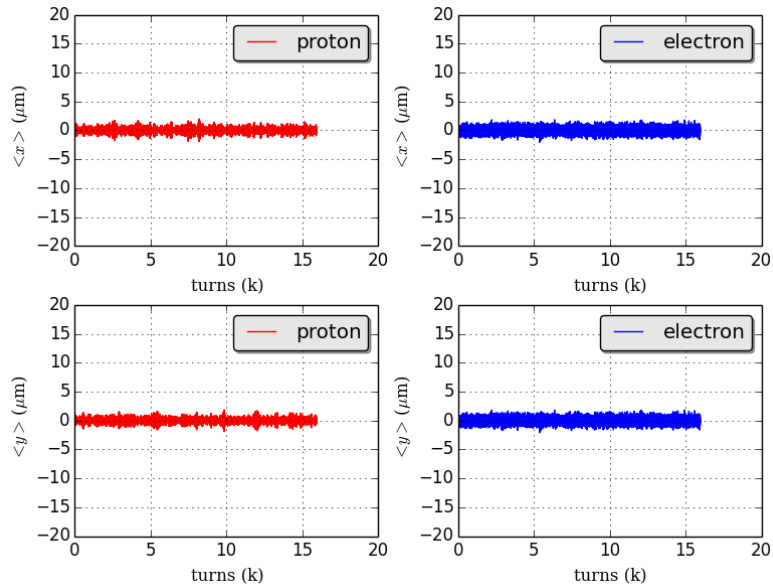
$\sigma_{\text{offs}} = 1\mu\text{m}$

$\sigma_{\text{offs}} = 2\mu\text{m}$



$g_{x,p} \approx 2.9 \mu\text{m/s}$, $g_{x,p} \approx 3.1 \mu\text{m/s}$

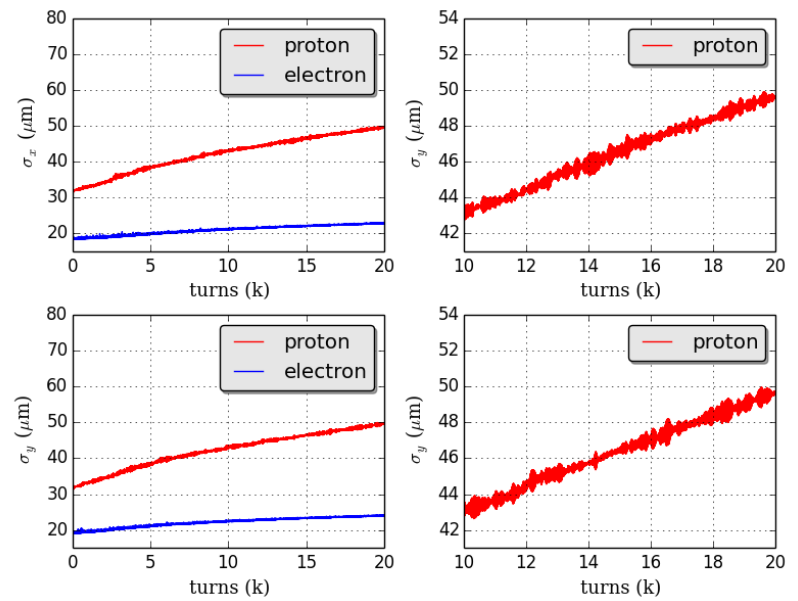
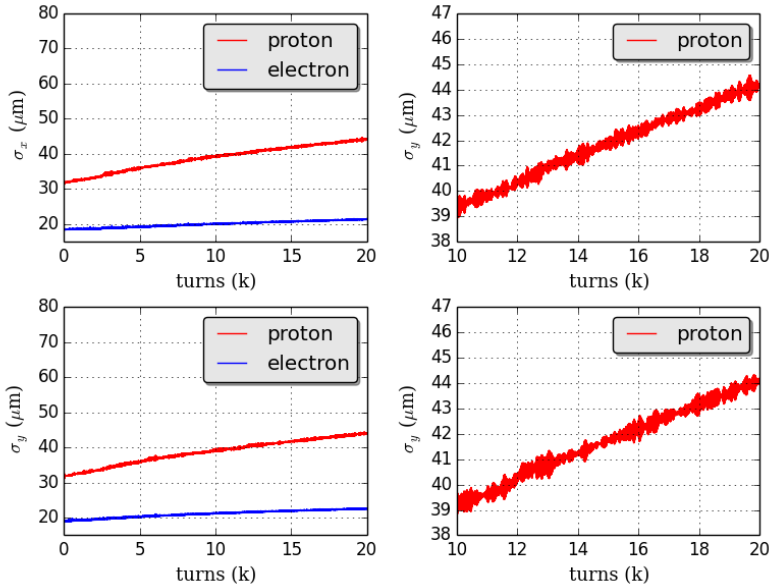
$g_{x,D} \approx 8.6 \mu\text{m/s}$, $g_{x,D} \approx 8.2 \mu\text{m/s}$



BBSS simulations with random offsets in e-beam

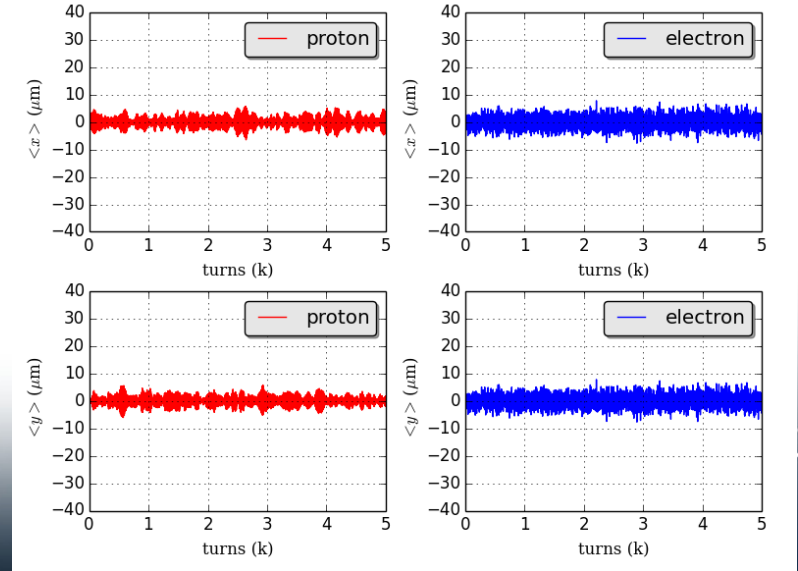
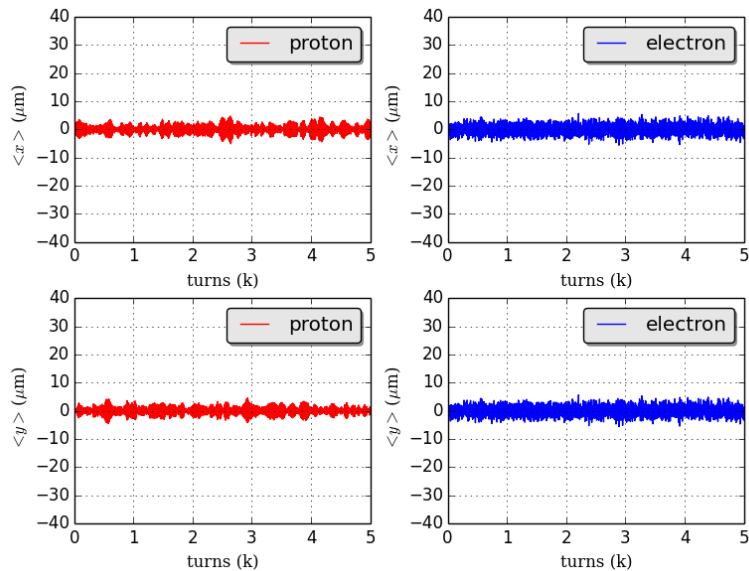
$\sigma_{\text{offs}} = 3\mu\text{m}$

$\sigma_{\text{offs}} = 4\mu\text{m}$



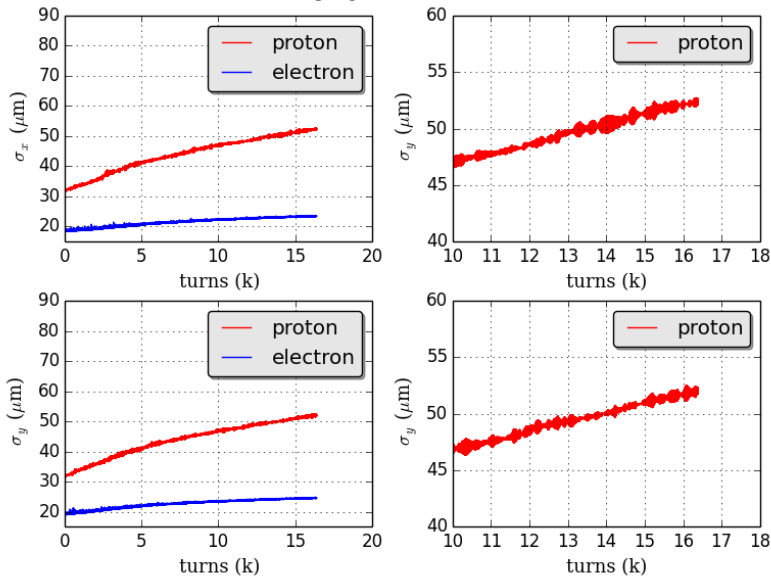
$g_{x,p} \approx 13.3 \mu\text{m/s}$, $g_{x,p} \approx 13.6 \mu\text{m/s}$

$g_{x,p} \approx 17.6 \mu\text{m/s}$, $g_{x,p} \approx 18.6 \mu\text{m/s}$

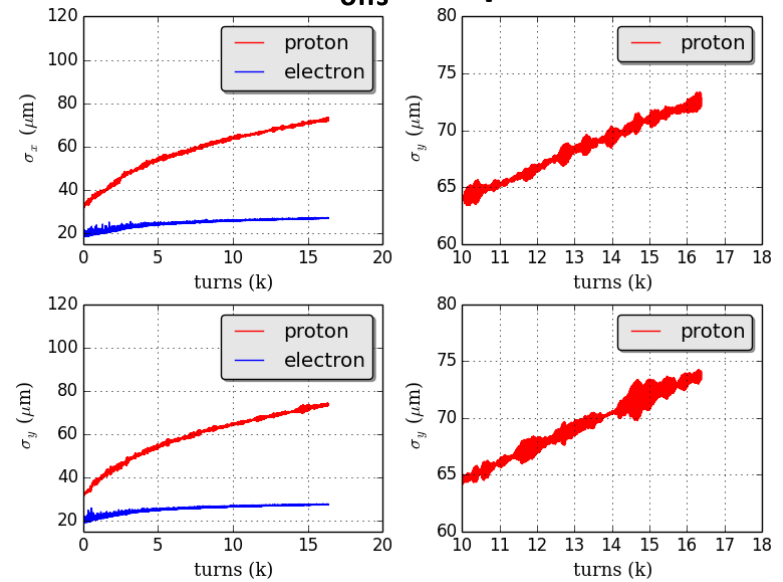


BBSS simulations with random offsets in e-beam

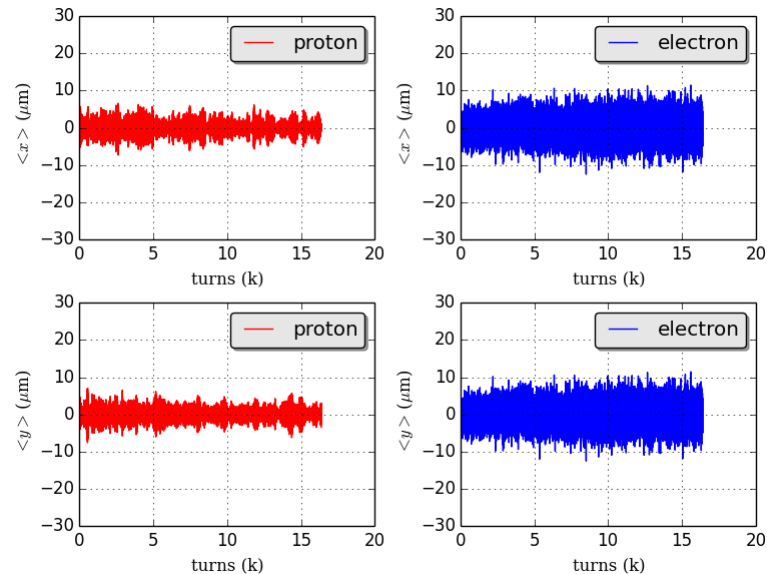
$\sigma_{\text{offs}} = 5\mu\text{m}$



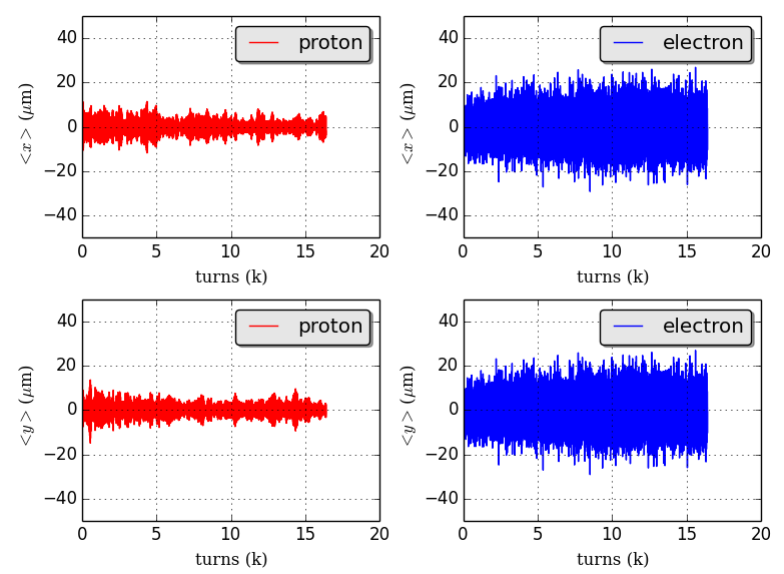
$\sigma_{\text{offs}} = 10\mu\text{m}$



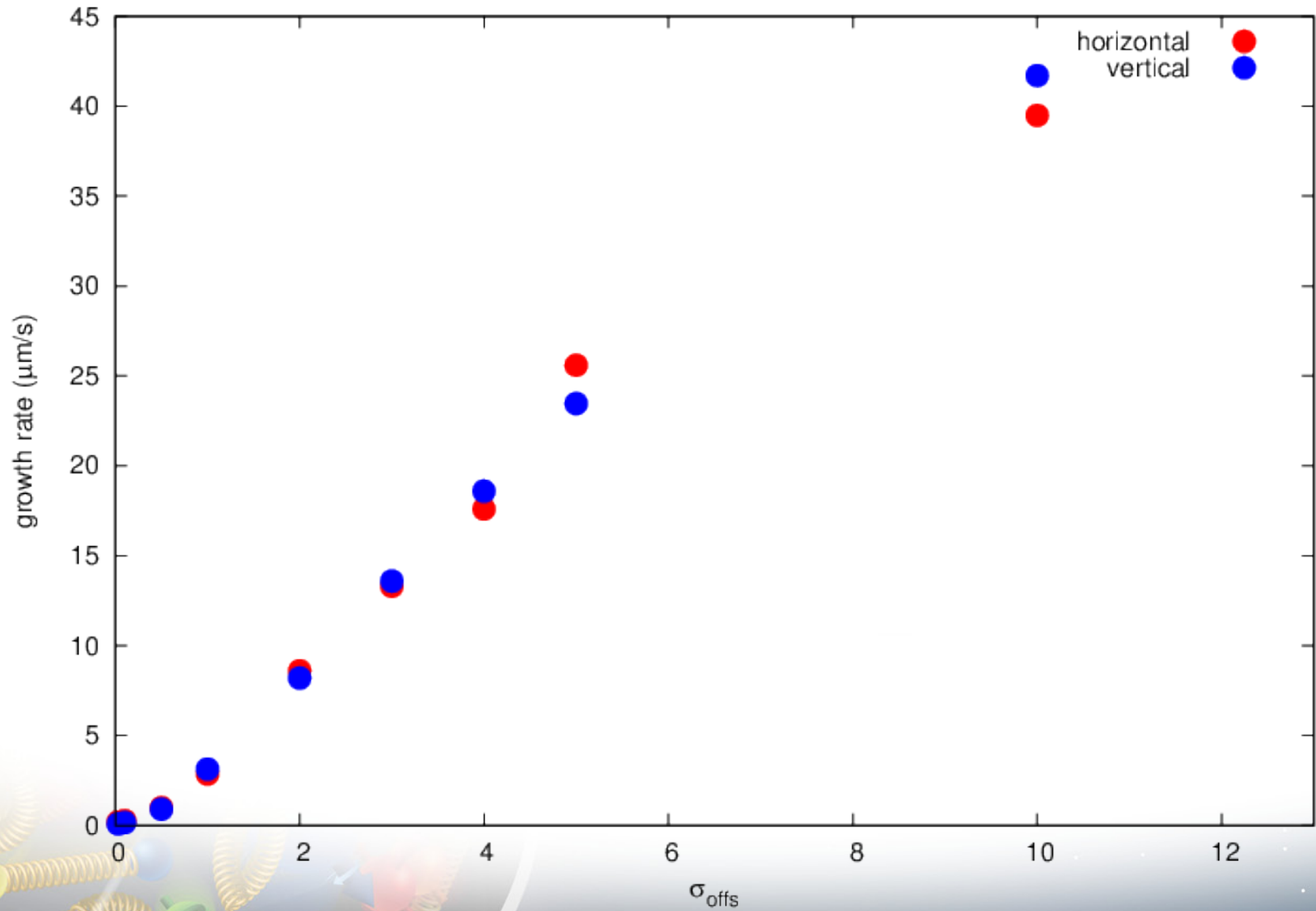
$g_{x,p} \approx 25.6 \mu\text{m/s}$, $g_{x,p} \approx 23.5 \mu\text{m/s}$



$g_{x,p} \approx 39.5 \mu\text{m/s}$, $g_{x,p} \approx 41.7 \mu\text{m/s}$

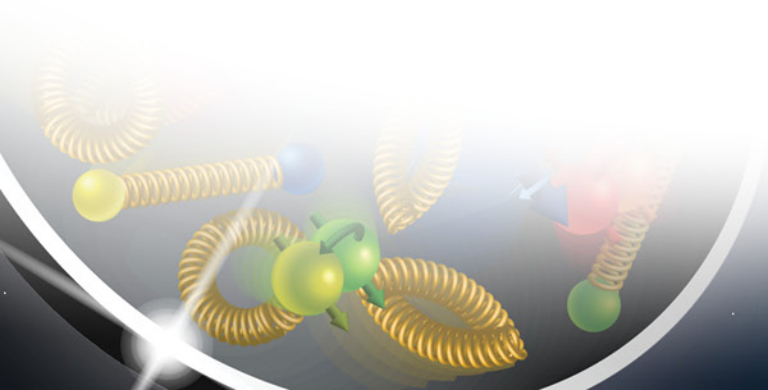


Proton Size Growth Rates

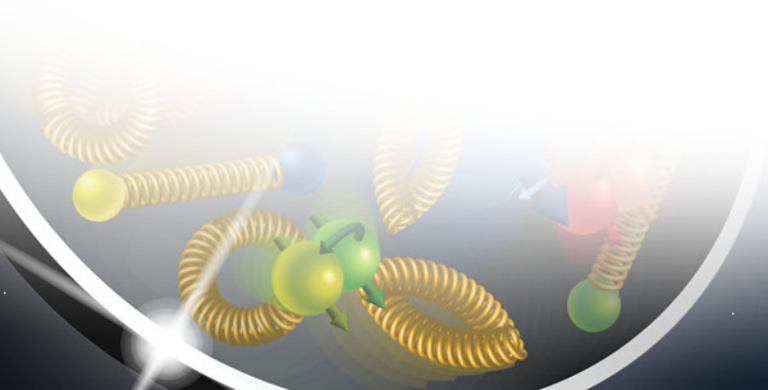


Discussion and Further Studies

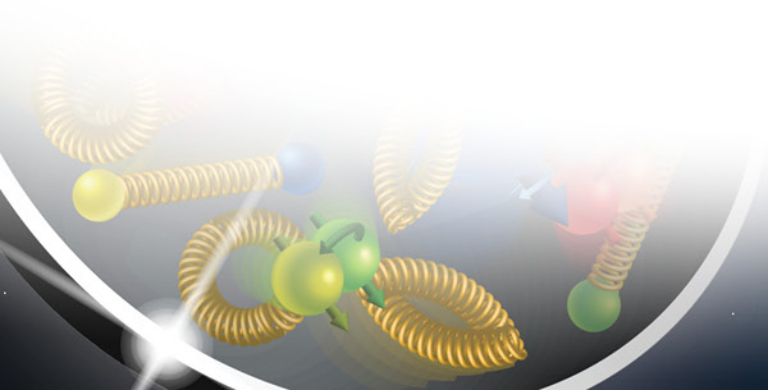
- Random offsets in electron bunches at the interaction point induce large proton size for $\sigma_{\text{offs}} > 0.03 \sigma_{x/y,p}$.
- Convergence/asymptotic studies are required to characterize the stability of the proton beam.
- Further studies will consider the impact of fluctuations in the electron bunch population on the stability of the proton beam.



Thank you for your attention!



Back Up Slides



Advantages & Disadvantages

Ring-Ring

- Proven technology (B-factory)
- Supports both electron and positron (!) beams options
- Requires significant (3-fold) increase to reach $L=0.8 \times 10^{33} \text{ cm}^{-2} \text{ sec}^{-1}$ but with very short ($\pm 1 \text{ m}$) detector
- Reasonable detector length ($\pm 3 \text{ m}$) reduces luminosity for present proton/ion intensities in RHIC below or about $10^{32} \text{ cm}^{-2} \text{ sec}^{-1}$
- Polarization is not available in forbidden energy zones
- Single IP (period).
- Machine element inside detector
- Luminosity plummets at lower E_{cm}

Linac-Ring

- High luminosity up to $10^{34} \text{ cm}^{-2} \text{ sec}^{-1}$
- Satisfy eRHIC physics goal with present proton/ion intensities in RHIC ($L > 10^{33} \text{ cm}^{-2} \text{ sec}^{-1}$)
- Allows multiple IPs
- No machine elements inside detector(s)
- No significant limitation on the lengths of detectors
- Allows wider range of CM-energies with high luminosities
- Full spin transparency at all energies
- Energy of ERL is simply upgradeable
- Novel technology
- Need R&D on polarized gun
- Needs a dedicated ring positrons (if required)

Documentation on Linac-Ring eRHIC

Physics Requirements

- To provide electron-proton and electron-ion collisions
- Energy ranges:
 - 2-10 GeV polarized e^- or 10 GeV polarized e^+
 - 26-250 GeV polarized protons or 100 GeV/u Au
- Luminosities:
 - $> 10^{33} \text{ cm}^{-2}\text{s}^{-1}$ region for e-p
 - $> 10^{31} \text{ cm}^{-2}\text{s}^{-1}$ region for e-Au
- $>70\%$ polarization degree for both lepton and proton beams
- Longitudinal polarization in the collision point

eRHIC

Zeroth-Order Design Report

BNL: L. Ahrens, D. Anderson, M. Bai, J. Beebe-Wang, I. Ben-Zvi, M. Blaskiewicz, J.M. Brennan, R. Calaga, X. Chang, E.D. Courant, A. Deshpande, A. Fedotov, W. Fischer, H. Hahn, J. Kewisch, V. Litvinenko, W.W. MacKay, C. Montag, S. Ozaki, B. Parker, S. Peggs, T. Roser, A. Ruggiero, B. Surrow, S. Tepikian, D. Trbojevic, V. Yakimenko, S.Y. Zhang
MIT-Bates: W. Franklin, W. Graves, R. Milner, C. Tschalaer, J. van der Laan, D. Wang, F. Wang, A. Zolfaghari and T. Zwart
BINP: A.V. Orboev, Yu.M. Shatunov
DESY: D.P. Barber

Editors: M. Farkhondeh (MIT-Bates) and V. Ptitsyn (BNL)

<http://www.agrhichome.bnl.gov/eRHIC/>

Goals for eRHIC

Appendix A of the eRHIC ZDR

Linac-Ring eRHIC.

Daniel Anderson, Ilan Ben-Zvi¹, Rama Calaga¹, Xiangyun Chang¹,
 Manouchehr Farkhondeh¹, Alexei Fedotov¹, J. rgKewisch¹, Vladimir Litvinenko¹,
 William Mackay¹, Christoph Montag¹, Thomas Roser¹, Vitaly Yakimenko¹
⁽¹⁾ C-AD, BNL ⁽²⁾ Bates, MIT ⁽³⁾ Physics Department, BNL

Content	page
1. Introduction to the Linac-Ring collider	173
1.1 Advantages of the ERL-based eRHIC	181
2. Main beam parameters and luminosity	183
3. Layout of the Linac-ring eRHIC	186
a. Energy recovery Linac	188
b. Polarized electron gun	204
c. Laser source for the polarized gun	209
d. The e-beam polarization and polarization transparency of the ERL lattice	214
e. Electron cooling	219
f. Integration with IP	223
g. Considerations of the experiments	231
h. Adjustment of collision frequency for variable hadron energies	233
4. Cost	235
5. R&D items	236
6. Future energy upgrades	240
7. Summary	242
8. Acknowledgements	243

The diagram illustrates the collision point of the Linac-Ring eRHIC. It shows an incident lepton (electron) and an incident hadron (proton) interacting via a virtual photon. The virtual photon can produce a dilepton pair or a quark-antiquark pair. The quark-antiquark pair can further interact to produce a nucleus fragment or a proton. The diagram also shows the production of a nucleus fragment and a proton from the collision of a virtual photon and a nucleus fragment.

BBSS simulations with no random offsets in e-beam

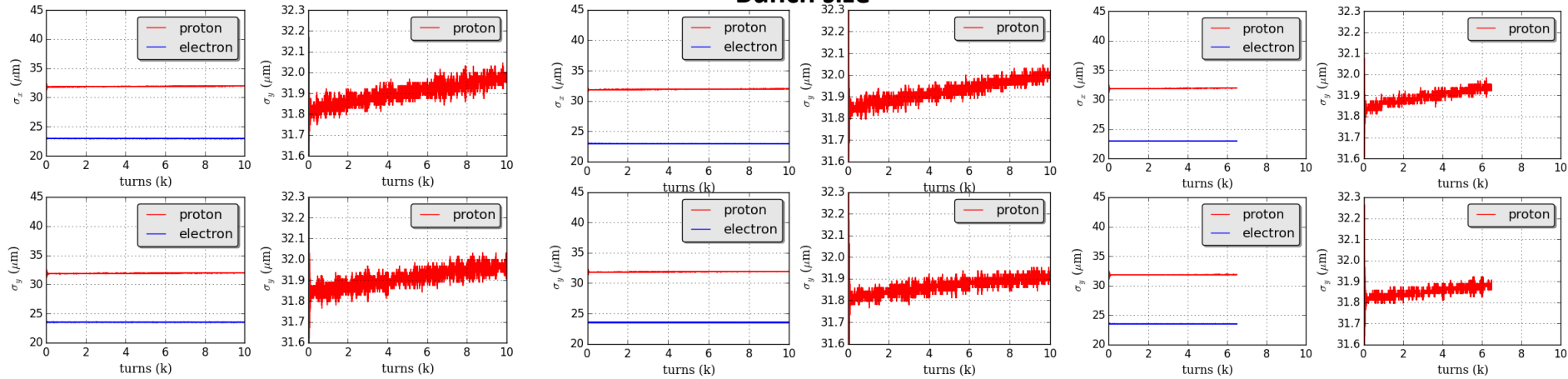
M # of macroparticles

$M_p = M_e = 500k$

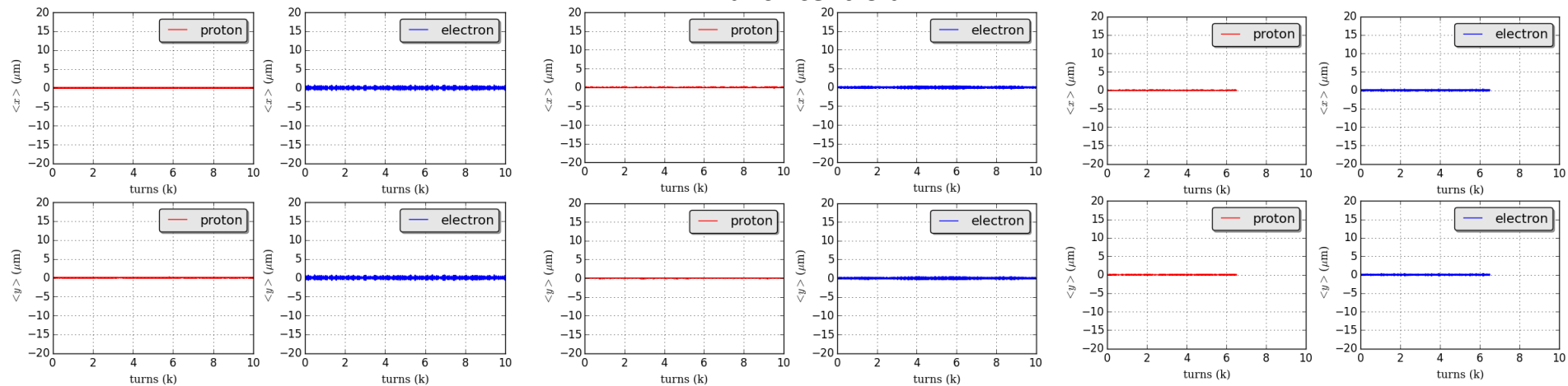
$M_p = N_e = 1M$

$M_p = M_e = 2M$

Bunch size

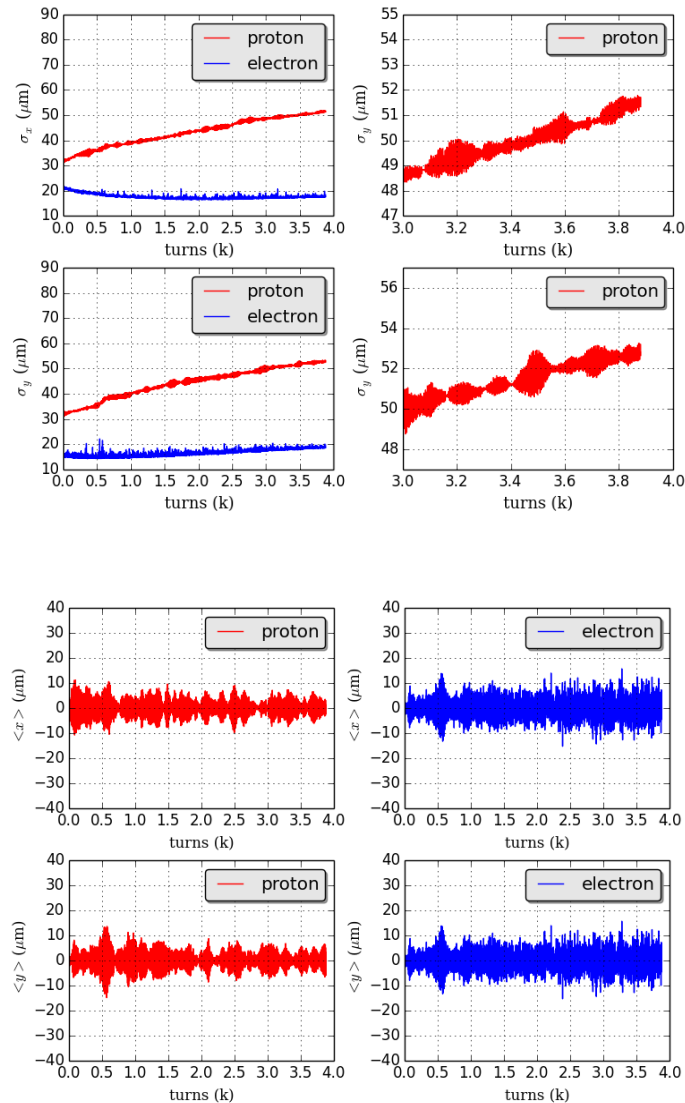


Bunch centroid



BBSS simulations with random offsets in e-beam

Rms offset 10 microm, N_p
=2



Rms offset 1 microm, $N_p = 2$

